eLIFE elifesciences.org

RESEARCH ARTICLE

Figures and figure supplements

A conserved quality-control pathway that mediates degradation of unassembled ribosomal proteins

Min-Kyung Sung *et al*

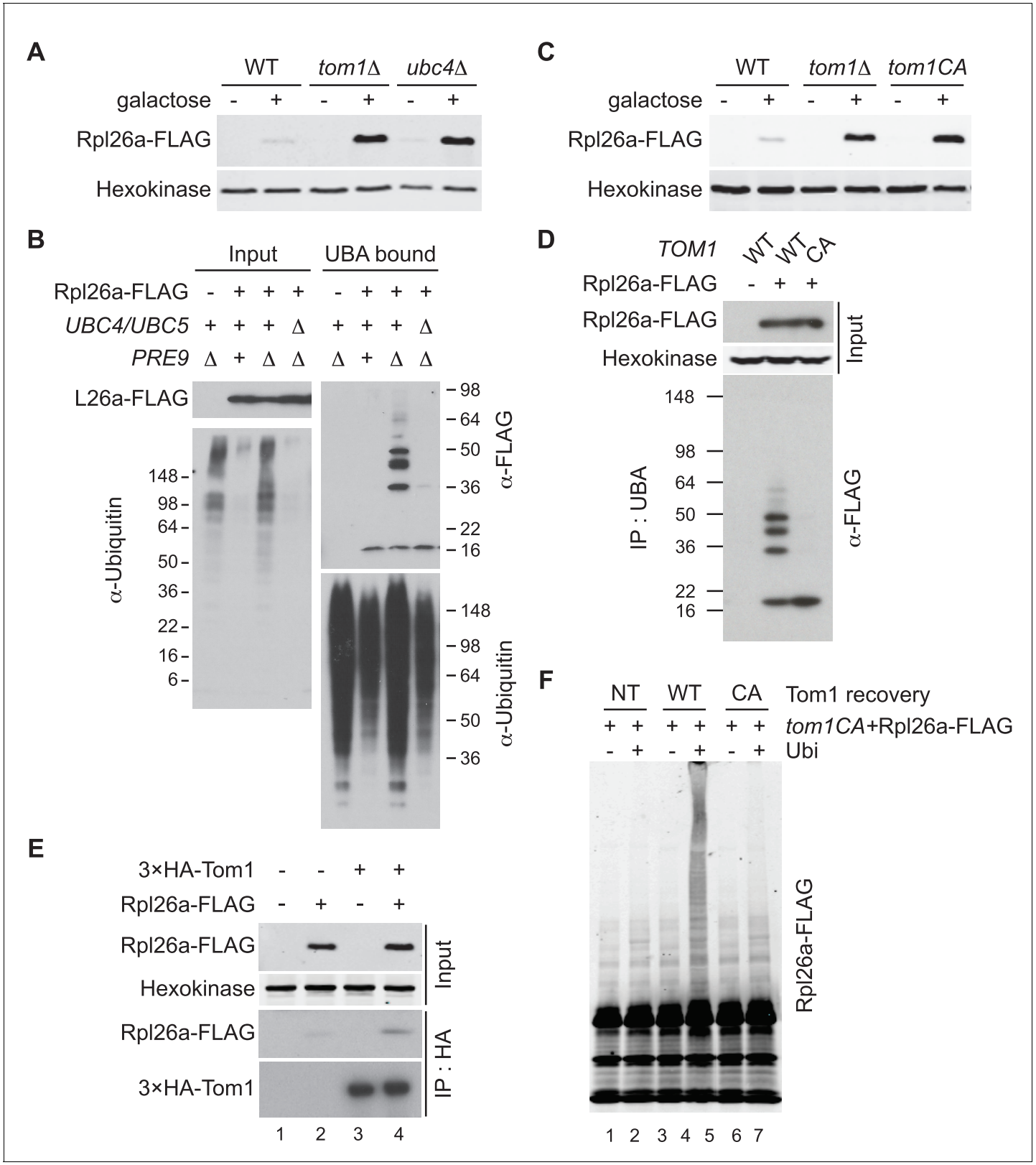

Figure 1. Ubc4/5 and Tom1 are the E2 and E3 enzymes responsible for ERISQ. (**A**) Rpl26a^{FLAG} accumulates in *tom1Δ* and *ubc4Δ*. Accumulation of Rpl26a^{FLAG} upon galactose induction in WT, *tom1Δ and ubc4Δ* cells was evaluated by SDS-PAGE and immunoblotting with the indicated antibodies. n = 3 biological replicates. (**B**) Rpl26a^{FLAG} ubiquitination depends on Ubc4/Ubc5. Rpl26a^{FLAG} was induced in cells of the indicated genotypes and cell

Figure 1 continued on next page

Figure 1 continued

lysates were prepared and subjected to pull-down with UBA domain resin. Input and bound proteins were evaluated as in (**A**). n = 3 biological replicates. (**C**) Rpl26a^{FLAG} accumulates in *tom1*^{CA} cells. As in (**A**) except that the Tom1 ligase-dead (*tom1*^{CA}) mutant was used. n = 3 biological replicates. (**D**) Rpl26a^{FLAG} ubiquitination depends on Tom1. As in (**B**) except that cells expressing WT Tom1 or Tom1^{CA} were treated with bortezomib for 45 min after addition of galactose. n = 3 biological replicates. (**E**) Rpl26a^{FLAG} binds ^{3xHA}Tom1. Anti-HA immunoprecipitates from cells expressing $^{3\times HA}$Tom1 and Rpl26a^{FLAG} were immunoblotted with antibodies to HA, FLAG, and hexokinase. n = 3 biological replicates. (F) In vitro ubiquitination of Rpl26a^{FLAG} by Tom1. Rpl26a^{FLAG} retrieved in ^{3xHA}Tom1^{CA} immunoprecipitates was supplemented or not with E1/E2/ubiquitin/ATP (Ubi) and Tom1 retrieved from untagged (NT), ^{3xHA}*TOM1* (WT), or ^{3xHA}*TOM1*^{CA} (CA) cells, as indicated. See detailed methods in Material and methods. n = 3 biological replicates.

DOI: 10.7554/eLife.19105.003

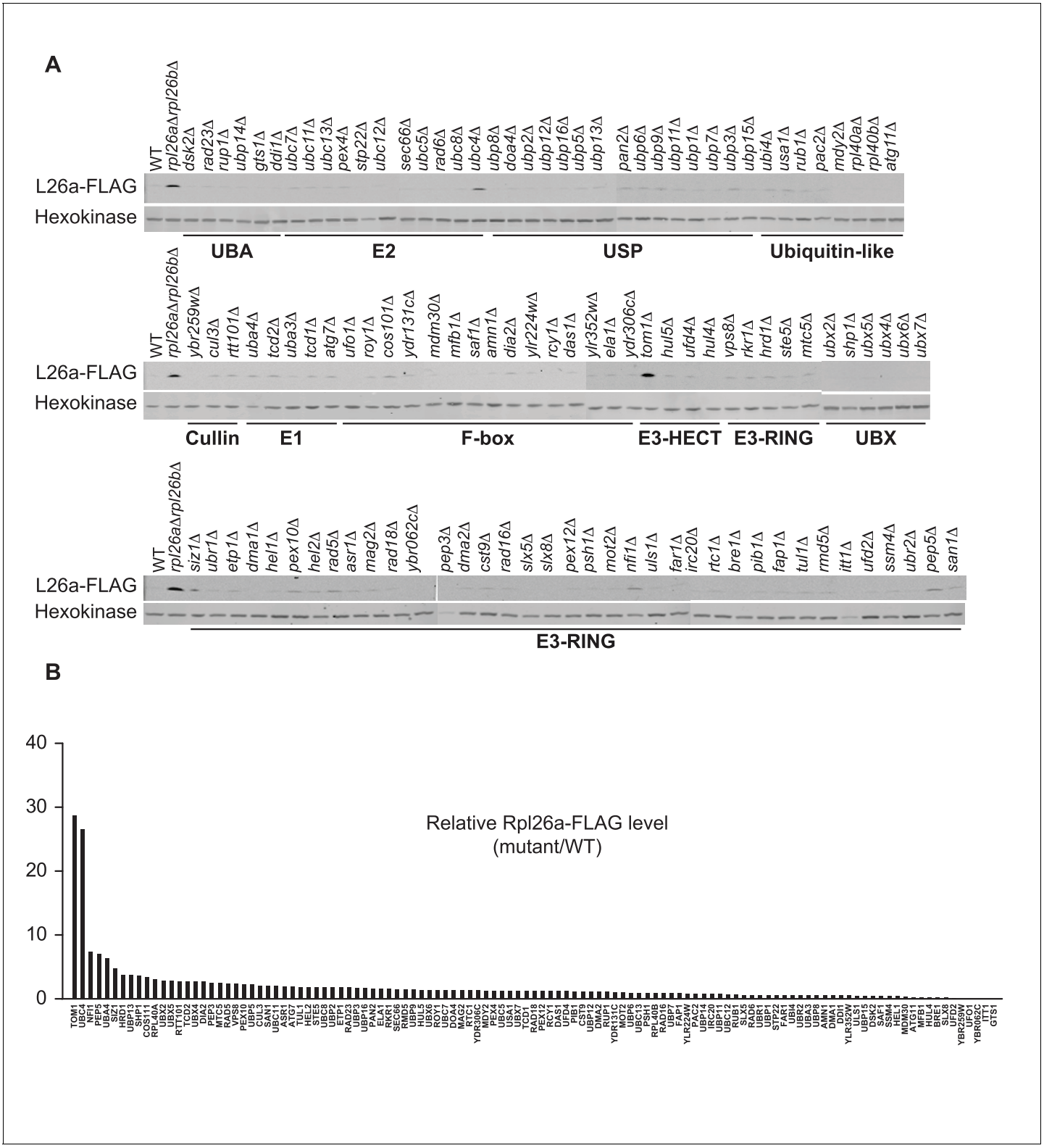

Figure 1—figure supplement 1. Identification of ERISQ defect in *tom1*Δ and *ubc4*Δ. (**A**) One hundred fifteen different knockout mutant strains each containing a plasmid that expressed Rpl26a^{FLAG} from the *GAL10* promoter were used. Rpl26a^{FLAG} induced in *rpl26a*Δ*rpl26b*Δ cells was used as a positive control. n = 1 biological replicate. (**B**) Quantification of data in (**A**).

DOI: 10.7554/eLife.19105.004

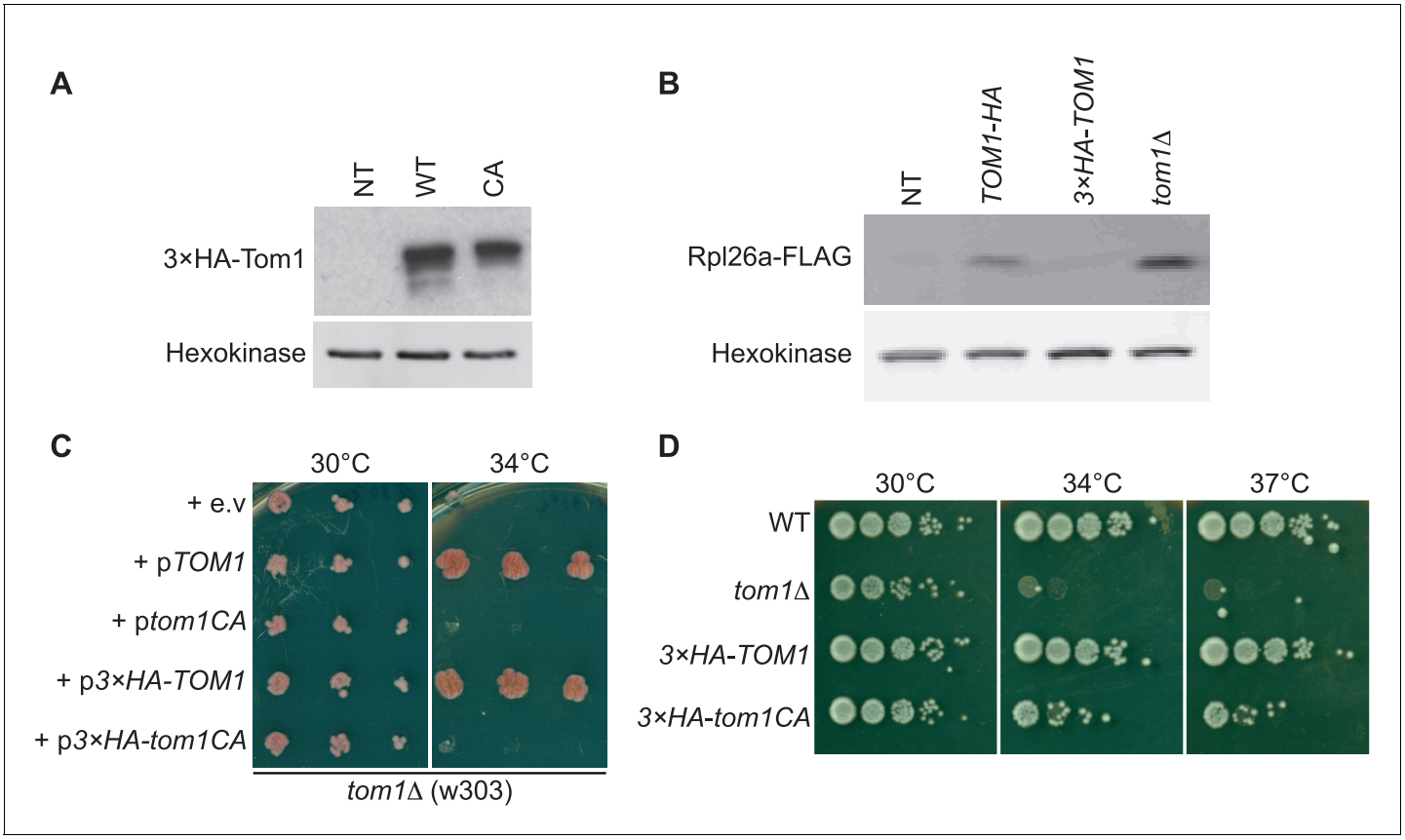

Figure 1—figure supplement 2. Characterization of tagged and ligase-dead Tom1. (**A**) Protein level of $^{3\times HA}$Tom1 in cells expressing Tom1 (NT), $^{3\times HA}$Tom1 (WT) and $^{3\times HA}$Tom1^{CA} (CA). n = 2 biological replicates. (**B**) Protein level of overexpressed Rpl26a^{FLAG} induced in cells expressing Tom1 (NT), Tom1$^{HA,\ 3\times HA}$Tom1 and *tom1*Δ. Note that a C-terminal tag on Tom1 compromises function, allowing for greater accumulation of galactose-induced Rpl26a^{FLAG}. n = 2 biological replicates. (**C**) Cells of the indicated genotypes were spotted on SC-TRP and incubated at 30˚C or 34˚C for 2 days. n = 2 biological replicates. (**D**) As in (**C**), except that cells of the indicated genotypes were spotted on YPD and incubated at the indicated temperatures for 2 days. n = 2 biological replicates.

DOI: 10.7554/eLife.19105.005

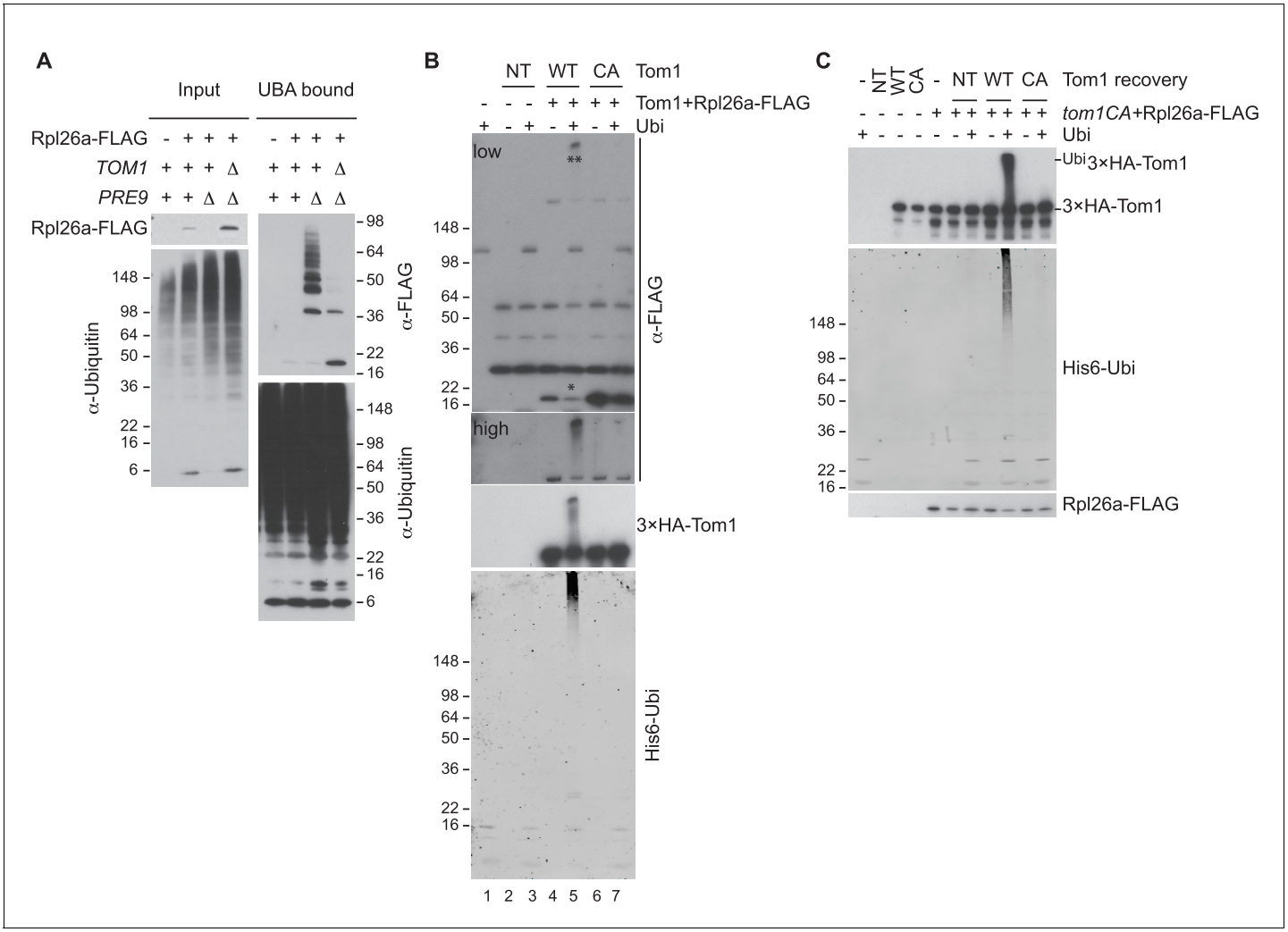

Figure 1—figure supplement 3. Tom1 mediates ubiquitination of overexpressed Rpl26a. (**A**) Polyubiquitination of Rpl26a^{FLAG}. Rpl26a^{FLAG} was induced in cells of the indicated genotypes and cell lysates were prepared and subjected to pull-down with UBA domain resin. Input and bound proteins were fractionated by SDS-PAGE and detected by immunoblot with the indicated antibodies. n = 2 biological replicates. (**B**) In vitro ubiquitination of Rpl26a^{FLAG} by Tom1. Lysates of cells expressing Rpl26a^{FLAG} and the indicated allele of ^{3xHA}Tom1 (NT is untagged control) were subjected to pull-down with anti-HA followed by addition of E1/E2/ubiquitin/ATP (Ubi) and incubation at 30°C for 1 hr. Reaction products were evaluated by immunoblot with the indicated antibodies. *indicates unmodified Rpl26a^{FLAG}. **indicate ubiquitinated Rpl26a^{FLAG}. Note the increase in ubiquitinated Rpl26a^{FLAG} (**) and the loss of unmodified Rpl26a^{FLAG} (*). n = 2 biological replicates. (**C**) Additional immunoblots of samples in ***Figure 1F***. n = 3 biological replicates.
DOI: 10.7554/eLife.19105.006

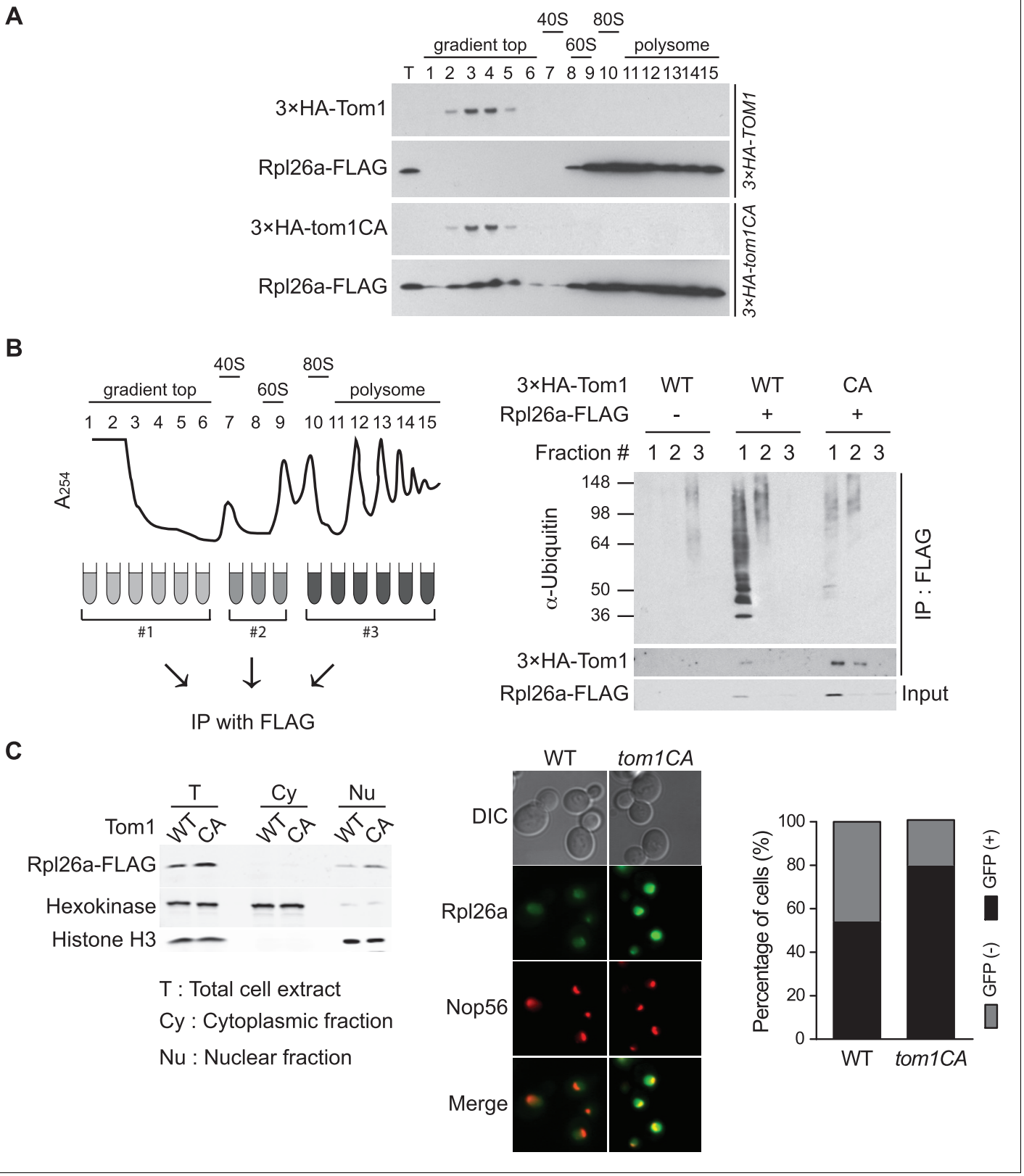

Figure 2. Tom1 functions in non-ribosomal fractions. (**A**) Sucrose gradient fractionation behavior of ^{3xHA}Tom1 and Rpl26a^{FLAG} upon galactose induction of Rpl26a^{FLAG} in $^{3\times HA}$*TOM1* or $^{3\times HA}$*TOM1*^{CA} cells. T indicates total extract. n = 2 biological replicates. (**B**) Tom1 is required for ubiquitination of

Figure 2 continued on next page

Figure 2 continued

unassembled Rpl26a^{FLAG}. Left: experimental scheme. Right: cells were treated with bortezomib for 30 min after induction of Rpl26a^{FLAG} with galactose and then lysed and fractionated as in panel A prior to being processed as depicted in panel B. n = 2 biological replicates. (**C**) Rpl26a accumulates in the nucleus of *tom1*^{CA} cells. Left: Subcellular fractionation of Rpl26a^{FLAG} induced in WT and *tom1*^{CA} cells. Histone H3 and Hexokinase were used as nuclear and cytoplasmic markers, respectively. CA refers to Tom1-Cys3235Ala. Right: Fluorescence microscopy of Rpl26a^{GFP} induced in WT and *tom1*^{CA} cells. Nop56-RFP marks nucleoli. Shown at far right is the percentage of GFP positive cells. n = 2 biological replicates.

DOI: 10.7554/eLife.19105.007

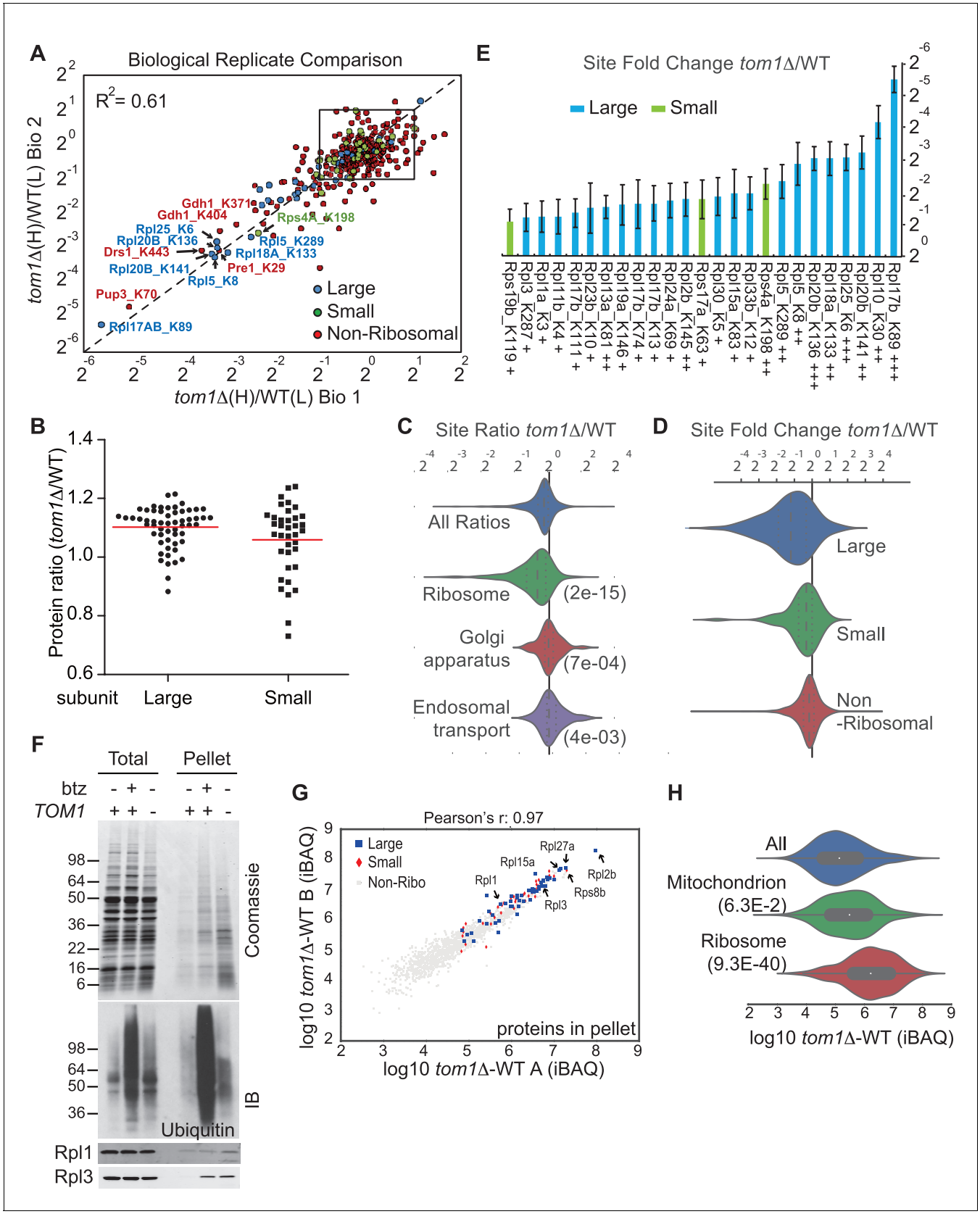

Figure 3. Diminished ubiquitination and accumulation of insoluble ribosomal proteins in *tom1* cells. (**A**) Diminished ubiquitination of ribosomal proteins in *tom1*Δ. Scatter plot of the SILAC ratios (*tom1*Δ/WT) for GlyGly-modified peptides identified in biological replicate 1 versus 2. Sites with the largest

Figure 3 continued on next page

Figure 3 continued

decrease in ubiquitination are annotated. The other pairwise comparisons are in ***Figure 3—figure supplement 2A***. n = 3 biological replicates. (**B**) Column scatter plot representing the distribution of ratios (*tom1*Δ/WT) for proteins of the large (circles) and small (square) ribosome subunits. A red bar indicates the mean. (**C**) Violin plot of gene ontology analysis of ubiquitinated proteins that had one or more ubiquitination site that decreased by ≥ 2-fold. The most strongly affected categories are shown. The number in parentheses refers to the disproportionate enrichment for the category in the top 10% of identifications and is the Benjamini and Hochberg corrected p-value from a Fisher Exact test. (**D**) Violin plot representing the distribution of ubiquitin site occupancy ratios (*tom1*Δ/WT) for the large (blue) and small (green) ribosome subunits, and non-ribosomal proteins (red). (**E**) The 25 ribosomal ubiquitination sites with the largest decrease in ubiquitin occupancy in *tom1*Δ. +++p<0.001; ++p<0.01; +p<0.05. Each site was observed in at least two of the three biological replicates. The error bars represent 95% confidence intervals. Note that ubiquitination at K37 and K69 in Rpl26b was decreased by 2.4-fold and 1.6-fold in *tom1*Δ, respectively (***Supplementary file 3B***). (**F, G**) Insoluble ribosomal proteins accumulate in *tom1*Δ. (**F**) Detergent-insoluble pellet fractions isolated from lysate (Total) of indicated cells were analyzed by SDS-PAGE and staining with Coomassie blue or immunoblotting with the indicated antibodies. The pellet fraction is overloaded 20-fold compared to the total and supernatant fractions. n = 2 biological replicates. (**G**) Scatter plot representing ΔiBAQ of biological replicate B *vs.* A for insoluble proteins in *tom1*Δ mutants. Ribosomal proteins with the largest increase in the pellet fraction upon *TOM1* deletion, and Rpl1 and Rpl3 are annotated. Pearson's r-value is indicated on top of the plot. The other pairwise comparisons are in ***Figure 3—figure supplement 3B***. n = 3 biological replicates. (**H**) Gene ontology analysis of proteins exhibiting increased insolubility in *tom1*Δ. Analysis is the same as for panel C.

DOI: 10.7554/eLife.19105.008

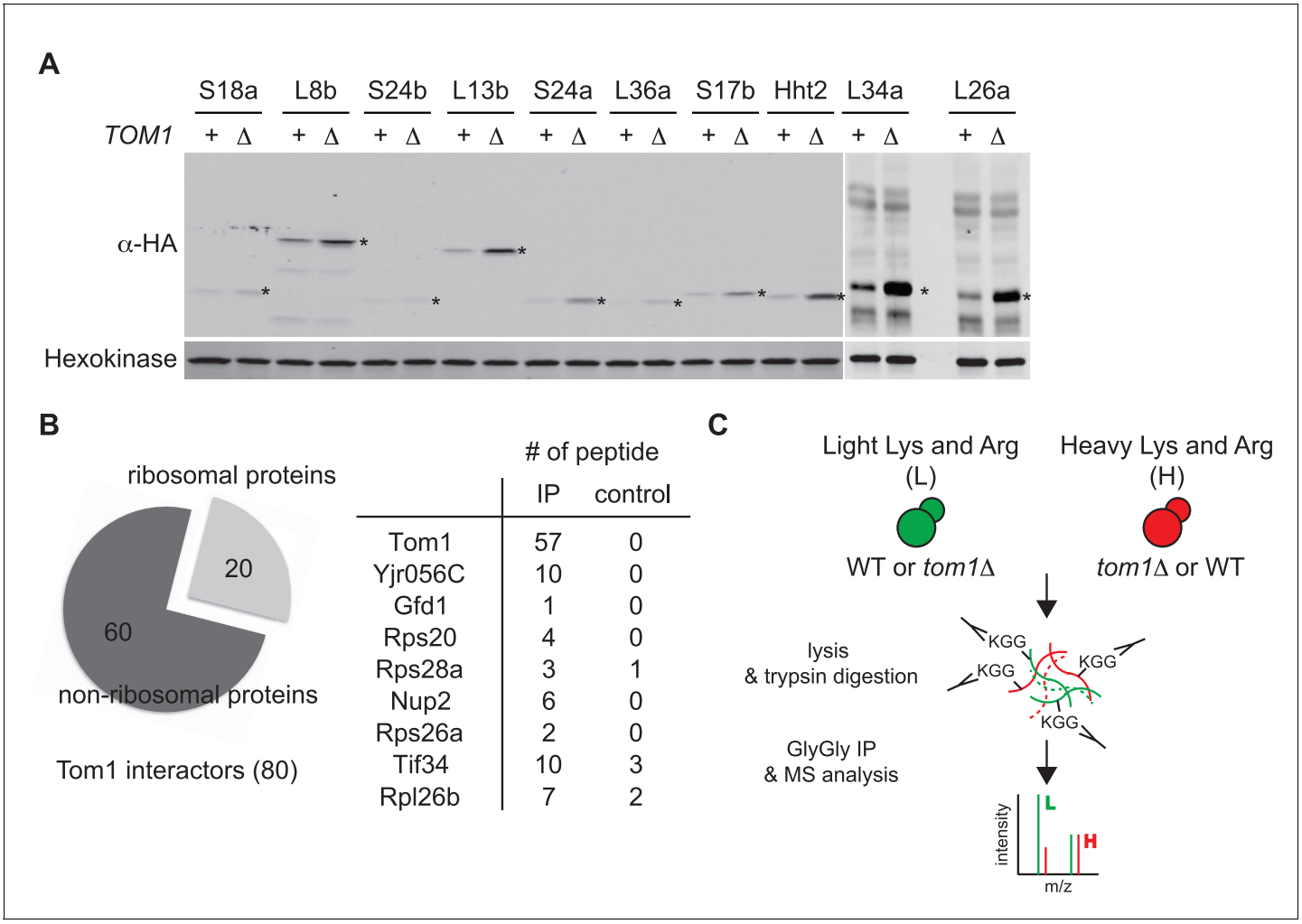

Figure 3—figure supplement 1. Tom1 targets a broad range of overexpressed and endogenous ribosomal proteins. (**A**) Relative levels of the transiently overexpressed, indicated ribosomal proteins (all tagged with a His6-HA-protein A ZZ domain epitope) in WT and *tom1*Δ mutants. n = 2 biological replicates. *indicates the expected size of protein. (**B**) Left: Cells expressing untagged-Tom1 or $^{3\times HA}$Tom1 were treated with bortezomib for 1 hr. Total cell extracts were adsorbed to HA resin and the bound fractions were analyzed by mass spectrometry. 80 proteins that increased >1.5 fold in $^{3\times HA}$Tom1 samples versus untagged samples were categorized into ribosomal or non-ribosomal proteins. Right: The number of peptides derived from the 9 proteins with the highest fold changes in $^{3\times HA}$Tom1 *vs.* untagged samples are shown. n = 1 biological replicate. (**C**) Schematic diagram of SILAC-based quantitative K-ε-GlyGly mass spectrometry (MS) strategy to identify Tom1-depdendent ubiquitination sites.

DOI: 10.7554/eLife.19105.009

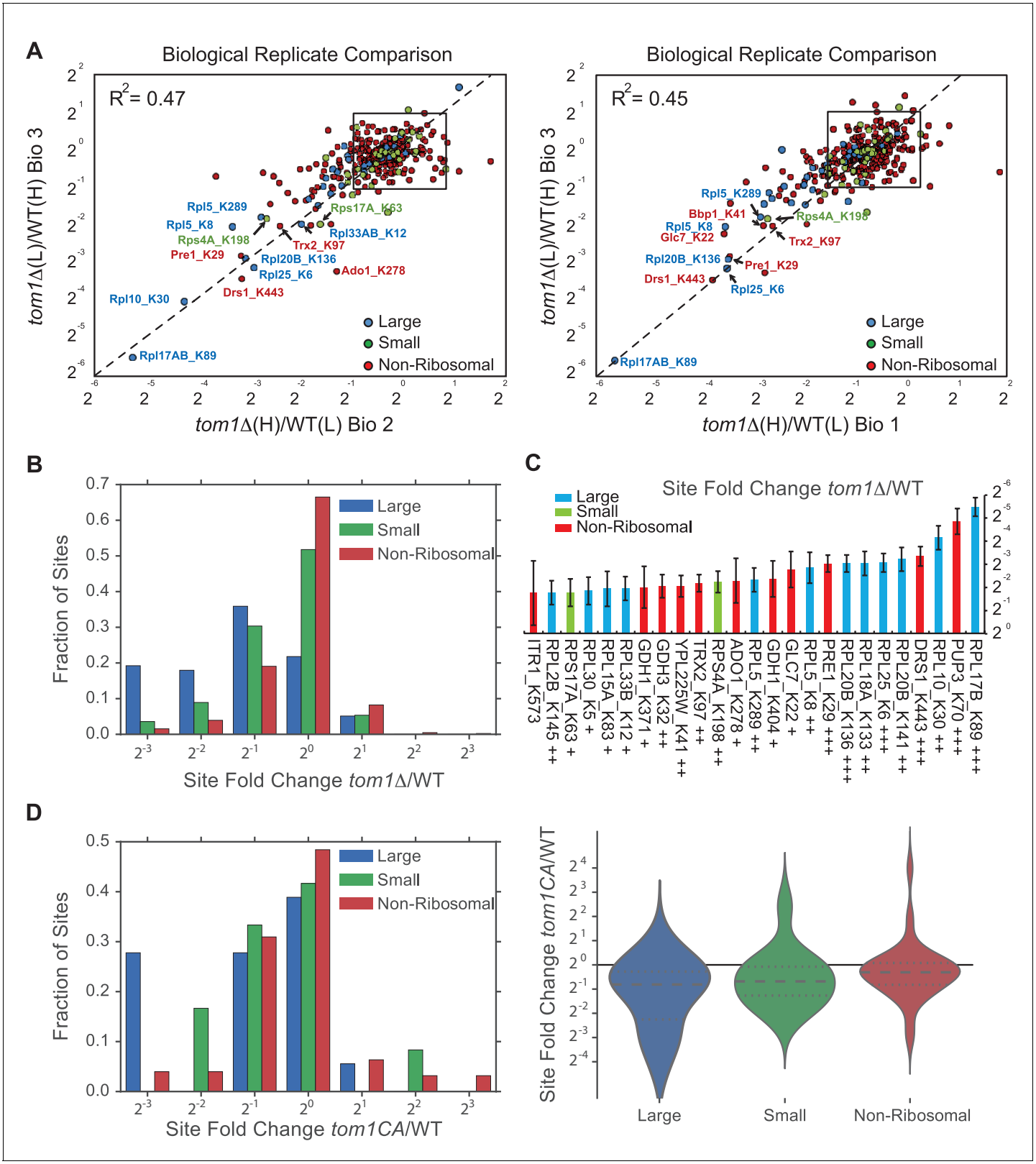

Figure 3—figure supplement 2. Quantitative GlyGly proteomic analyses of *tom1* mutants. (**A**) Scatter plots of the SILAC ratios (*tom1*Δ/WT) of biological replicate 3 *vs.* 2 (left) and biological replicate 3 *vs.* 1 (right) for GlyGly-modified peptides in *tom1*Δ and WT cells. Sites with the largest decrease in ubiquitination are annotated. These data accompany ***Figure 3A***. n = 3 biological replicates. (**B**) Histogram of *tom1*Δ/WT ubiquitination site

Figure 3—figure supplement 2 continued on next page

Figure 3—figure supplement 2 continued

ratios for ribosomal proteins of the large and small subunits, and non-ribosomal proteins. For each protein category, the fraction of total with a given ratio is plotted. (**C**) The 25 ubiquitination sites with the largest decrease in ubiquitin occupancy in *tom1Δ*. +++p<0.001; ++p<0.01: +p<0.05. Each site was observed in at least two of the three biological replicates. The error bars represent 95% confidence intervals. (**D**) Left: same as (B), except that a *tom1*^{CA} mutant was used instead of *tom1Δ*. Right: violin plot representing the distribution of ubiquitin site occupancy ratios for ribosomal proteins of the large (blue) and small (green) subunit, and non-ribosomal proteins (red). n = 3 biological replicates.

DOI: 10.7554/eLife.19105.010

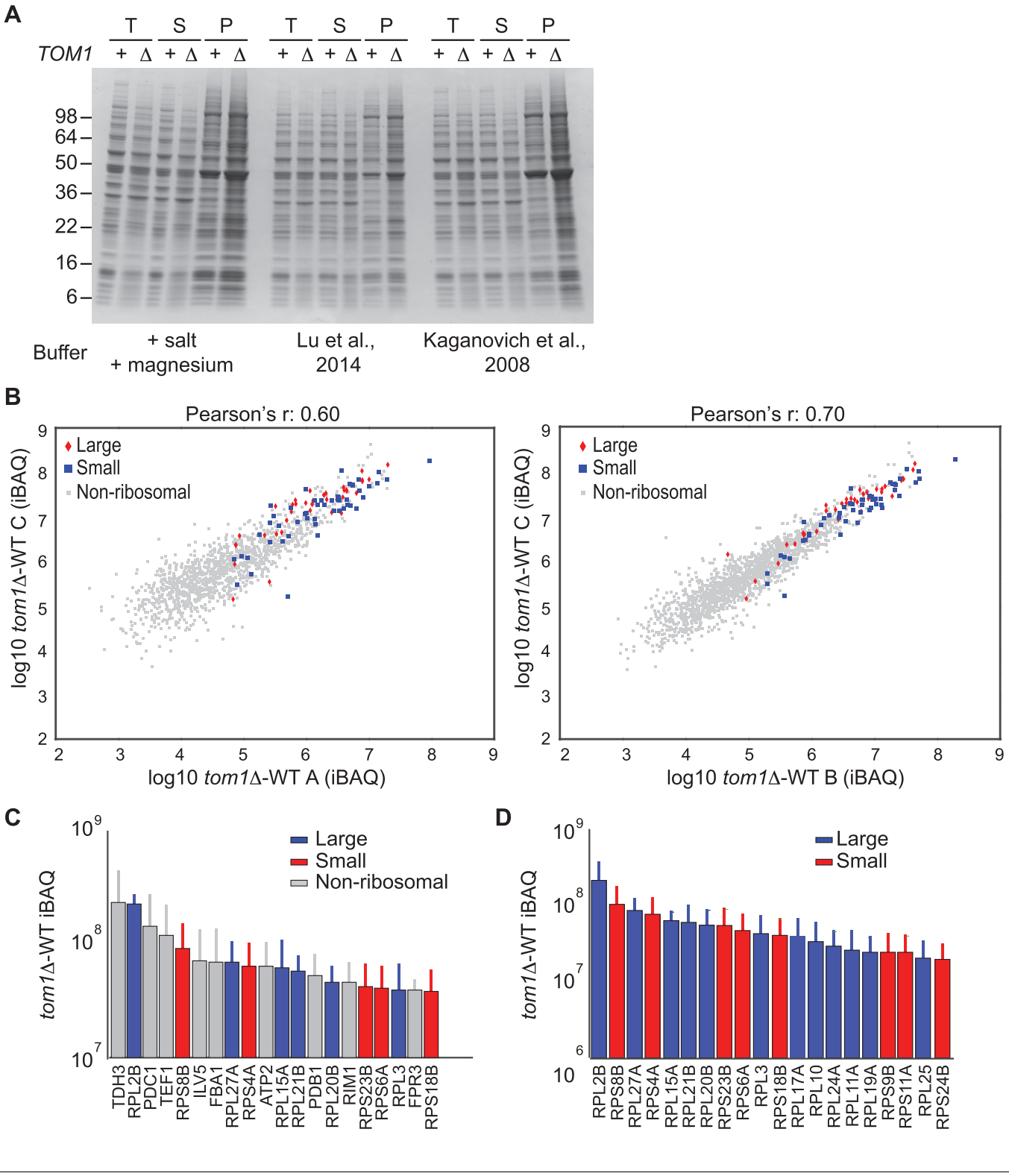

Figure 3—figure supplement 3. Endogenous ribosomal proteins accumulate as insoluble species in *tom1*Δ mutants. (**A**) Accumulation of insoluble proteins in *tom1* mutant cells is independent of lysis method or buffer. Cells of the indicated genotypes were lysed with glass beads in the presence of 3 different lysis buffers as indicated below gel image, and fractionated into detergent-soluble and insoluble fractions. Samples were separated by SDS-

Figure 3—figure supplement 3 continued on next page

Figure 3—figure supplement 3 continued

PAGE and stained with Coomassie Blue. The pellet fraction is overloaded 10-fold compared to the total and supernatant fractions. n = 2 biological replicates. T, S and P indicates total, soluble and pellet fractions, respectively. Note that results shown here are qualitatively similar to results in ***Figures 3F*** and ***6D–G***, even though the method employed to generate those figures employed lysis of spheroplasts in an EDTA-containing buffer. The reason for the higher background in this panel relative to the others is that the pellet fractions were not washed prior to analysis. (**B**) Scatter plots representing the ΔiBAQ of biological replicate C *vs.* A (left) and biological replicate C *vs.* B (right) for insoluble proteins in *tom1*Δ mutants. Pearson's r-value is indicated on top of the plot. These data accompany ***Figure 3G***. n = 3 biological replicates. (**C**) The 20 proteins with the largest increase in the pellet fraction upon *TOM1* deletion. Bars represent the average ΔiBAQ values with error bars indicating the standard error of the mean (SEM). (**D**) Same as (**C**), except the top 20 ribosomal proteins are shown.

DOI: 10.7554/eLife.19105.011

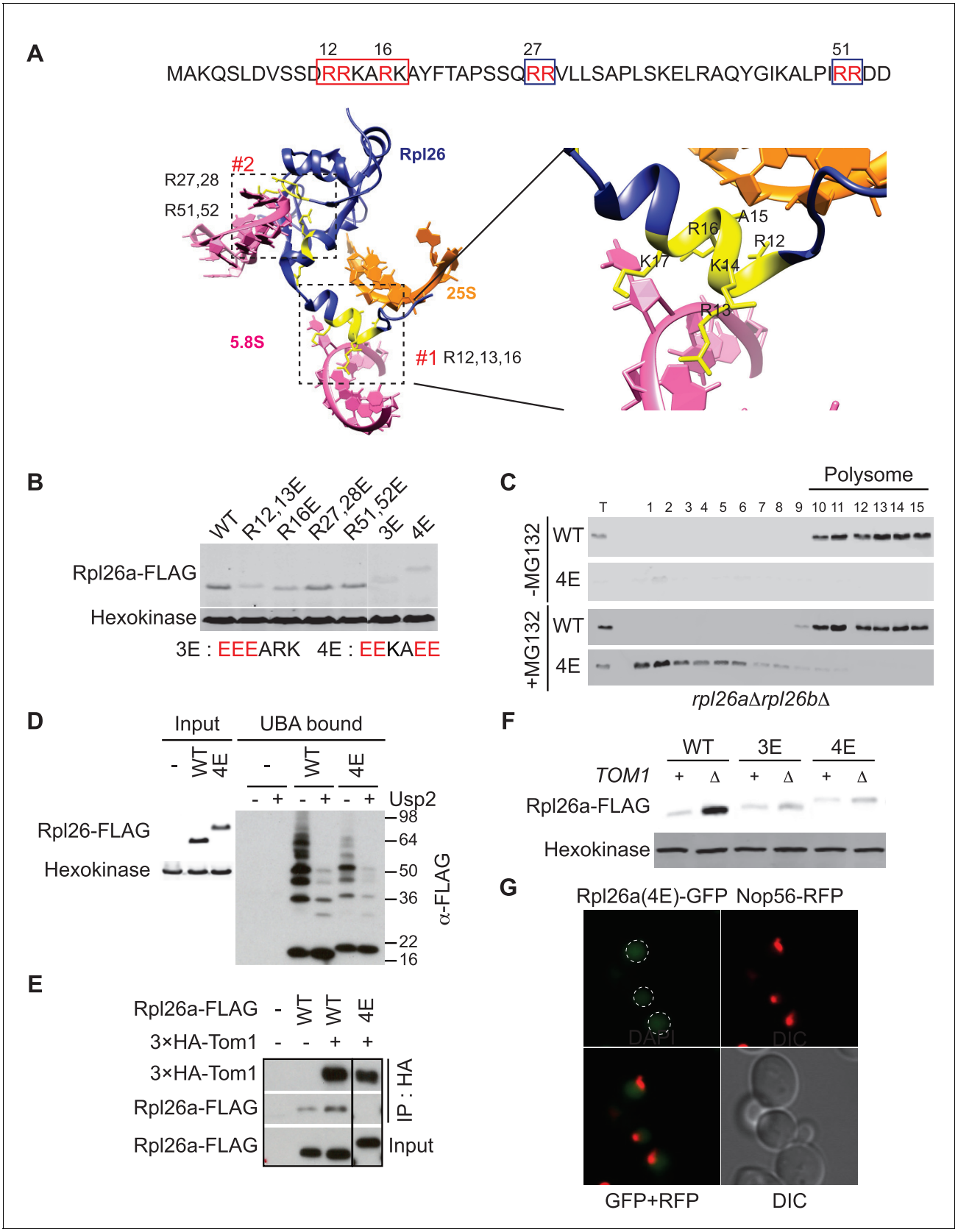

Figure 4. A short stretch of positively-charged residues in Rpl26a that mediates rRNA binding promotes association with Tom1. (**A**) Top: The first 54 amino acids of Rpl26a. Sequences adjacent to rRNA are boxed. Arginine residues targeted for mutation are in red. Bottom: Relative positions of

Figure 4 continued on next page

Figure 4 continued

arginines and rRNA based on the atomic model of the yeast 80S ribosome (PDB files 3U5D and 3U5E). Orange and pink ribbons correspond to 25S and 5.8S rRNA, respectively. Blue ribbon corresponds to Rpl26. Predicted regions (#1 and #2) for rRNA binding are highlighted in yellow and boxed. (**B**) Differential accumulation of WT and mutant Rpl26a^{FLAG} upon galactose induction. n = 2 biological replicates. (**C**) Top: Ribosome assembly of WT Rpl26a^{FLAG} or Rpl26a-4E^{FLAG} induced in *rpl26aΔrpl26bΔ* cells. Bottom: Same as above except that MG132 was added 30 min after addition of galactose. T indicates total extract. n = 2 biological replicates. (**D**) Polyubiquitination of Rpl26a-4E^{FLAG}. Assay was performed as described for ***Figure 1D***. Samples in '+' lanes were treated with deubiquitinating enzyme Usp2 prior to processing for SDS-PAGE, to demonstrate that high MW species were modified with ubiquitin. n = 2 biological replicates. (**E**) The Rpl26-4E mutation disrupts binding to Tom1. Lysates from cells of the indicated genotypes were subjected to pull-down with anti-HA followed by SDS-PAGE and immunoblotting for the indicated proteins. n = 2 biological replicates. (**F**) Protein level of Rpl26a^{FLAG} mutants upon galactose induction in WT and *tom1Δ* cells. n = 2 biological replicates. (**G**) Fluorescence images of Rpl26a^{4E}-GFP induced in WT cells. Nop56-RFP marks nucleoli. Dashed circles indicate nuclear region as judged by DAPI staining. n = 2 biological replicates.

DOI: 10.7554/eLife.19105.012

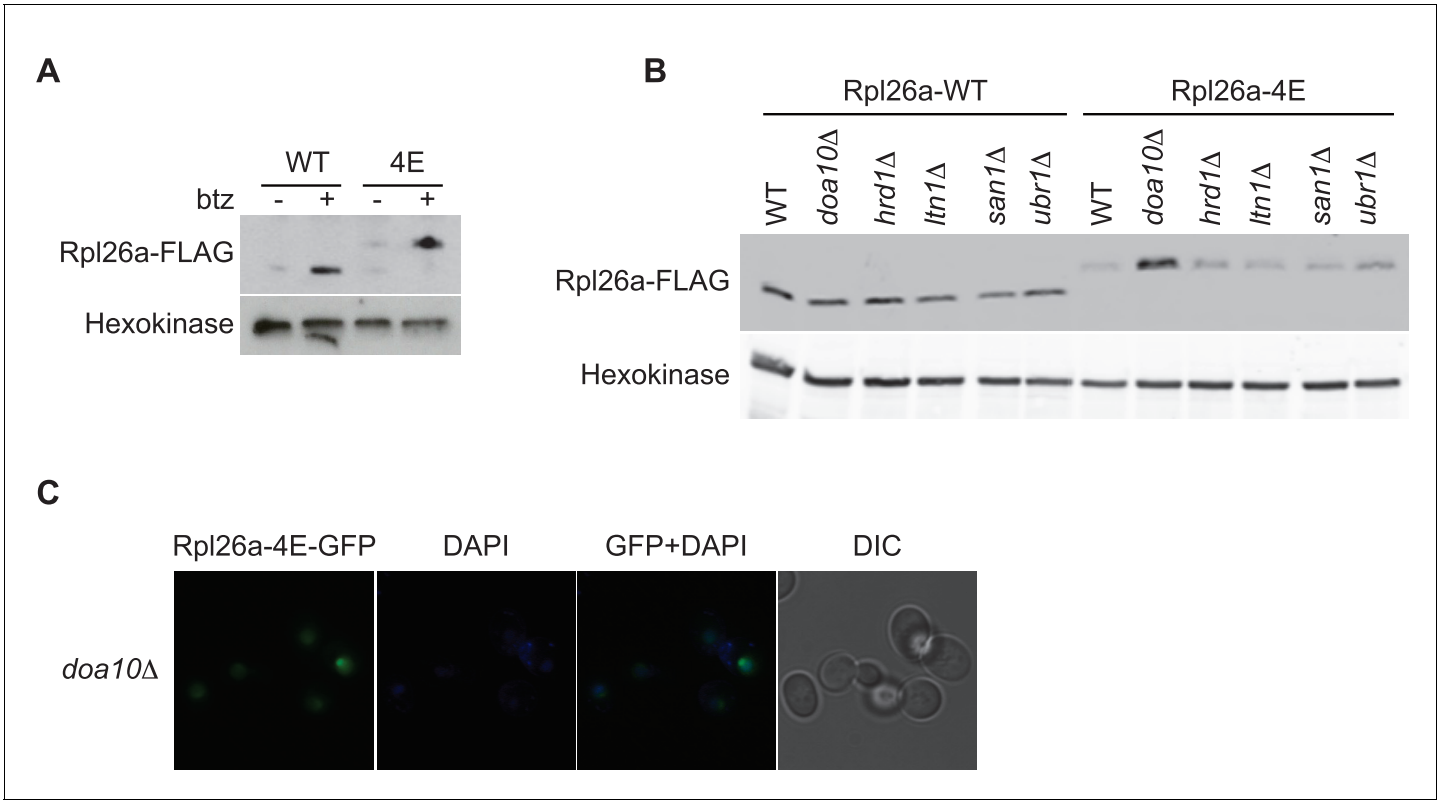

Figure 4—figure supplement 1. Rpl26a-4E mutant is unstable and degraded by Doa10 in the nucleus/nucleolus. (**A**) Similar accumulation of $Rpl26a^{FLAG}$ and $Rpl26a\text{-}4E^{FLAG}$ upon galactose induction in the presence of bortezomib. Total cell lysates were evaluated by SDS-PAGE and immunoblotting with the indicated antibodies. n = 1 biological replicate. (**B**) Differential accumulation of WT and Rpl26a-4E upon galactose induction in WT and known PQC mutants was evaluated by SDS-PAGE and immunoblotting with the indicated antibodies. n = 1 biological replicate. (**C**) Fluorescence images of $Rpl26a\text{-}4E^{GFP}$ induced in *doa10*Δ cells. n = 2 biological replicates.
DOI: 10.7554/eLife.19105.013

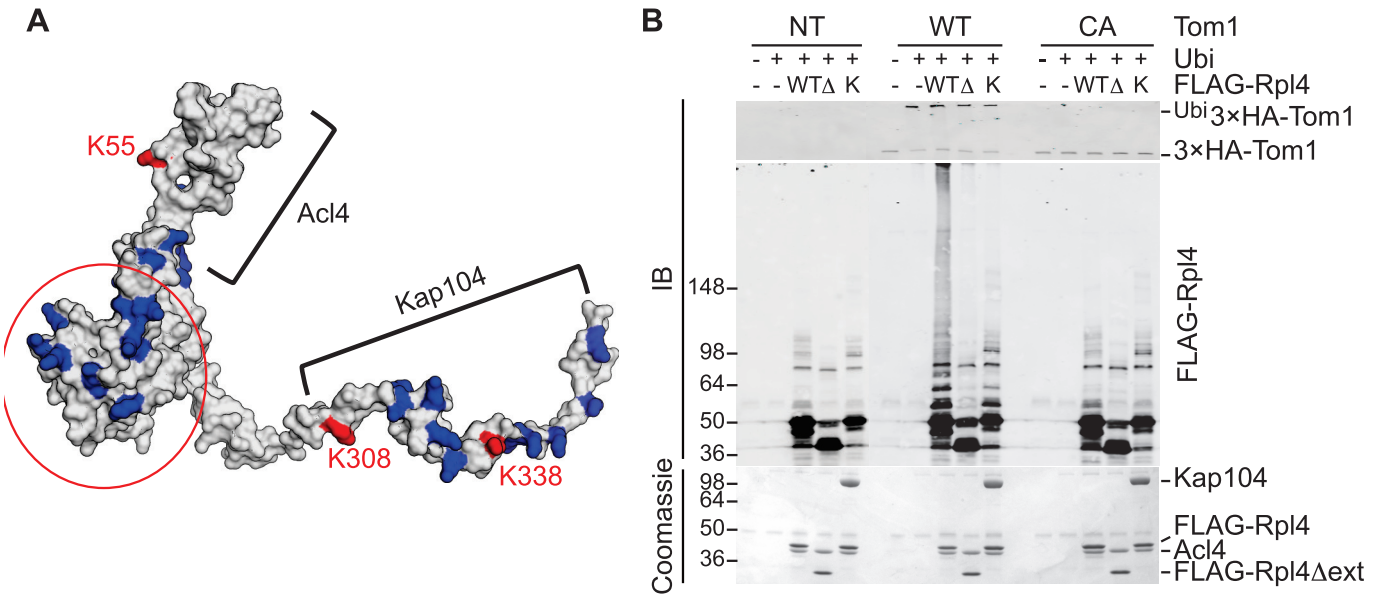

C

RP_Lys	Comments
Rpl2_K145, Rpl5_K8, Rpl15_K83, Rpl17_K74, Rpl17_K89, Rpl23_K10, Rpl33_K12	Inaccessible (7 lysines)
Rpl3_K287, Rpl17_K13, Rpl17_K111	Accessible (3 lysines)
Rpl5_K289, Rpl13_K81, Rpl18_K133, Rpl19_K146, Rpl20_K136, Rpl20_K141, Rpl10_K30*, Rpl24_K69*	Exposed but not accessible to 25 Å probe (8 lysines) * exposed in 60S but not 80S

Figure 5. Tom1 acts through residues that are normally inaccessible in the structure of the mature ribosome. (**A**) Structure of Rpl4 within the mature ribosome (PDB ID 4V88). Lysine residues are colored blue, with K55, K308, and K338 colored red. Areas involved in binding Acl4 and *ct*Kap104 are indicated. The exact boundaries of the Kap104 binding site are not known. The globular central domain, which is fully exposed in the ternary Acl4–Rpl4–Kap104 complex but is not ubiquitinated, is circled in red. (**B**) Ubiquitination of Acl4–Rpl4 by ^{3xHA}Tom1. Anti-HA immunoprecipitates from untagged (NT), ^{3xHA}*TOM1* (WT), and ^{3xHA}*tom1*^{CA} (CA) cells were supplemented or not with E1/E2/ubiquitin/ATP (Ubi) and purified Acl4–^{FLAG}Rpl4, Acl4-^{FLAG}Rpl4Δext and Acl4–^{FLAG}Rpl4–*ct*Kap104 proteins. Samples were analyzed by SDS-PAGE and staining with Coomassie blue or immunoblotting with the indicated antibodies. WT, Δ, and K refer to Acl4–^{FLAG}Rpl4, Acl4-^{FLAG}Rpl4Δext and Acl4–^{FLAG}Rpl4–*ct*Kap104, respectively. See detailed methods in Material and methods. n = 3 biological replicates. (**C**) Tom1 preferentially targets lysines that are inaccessible in mature ribosomes. Lysine residues shown are those from large subunit ribosomal proteins in ***Figure 3E*** that are incorporated in the model for the structure of the yeast ribosome (pdb 4V88). The structure of a HECT domain–donor ubiquitin complex (pdb 4LCD) predicts that a gap of radius 25 Å must be present for Tom1 to access a lysine for ubiquitination. Two of the sites (Rpl10 K30 and Rpl24 K69) are accessible in the 60S large subunit but become inaccessible upon formation of the 80S ribosome.

DOI: 10.7554/eLife.19105.014

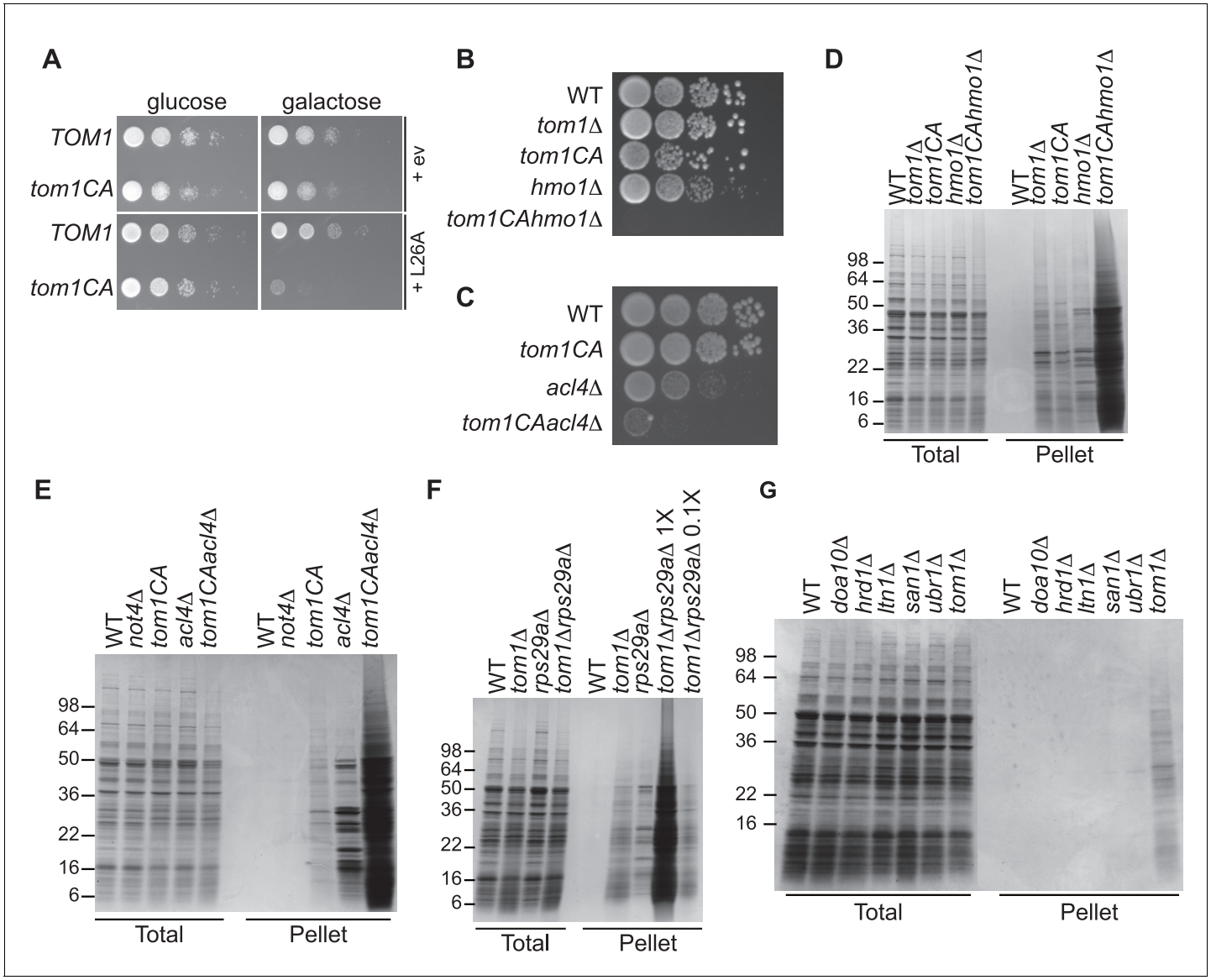

Figure 6. Defective ribosome assembly homeostasis and proteostatic collapse in *tom1* mutant cells. (**A–C**) Hypersensitivity of *tom1*^{CA} cells to imbalances in ribosome components. (**A**) Cells of the indicated genotypes were spotted in serial 10-fold dilutions on glucose or galactose medium and incubated at 30°C for 2 days. ev refers to empty vector. n = 2 biological replicates. (**B, C**) As in (**A**) except that cells of the indicated genotypes were spotted on YPD. n = 2 biological replicates. (**D–G**) Massive accumulation of insoluble proteins in *tom1* mutant cells. Cells of the indicated genotypes were lysed and fractionated into detergent-soluble and insoluble fractions, which were separated by SDS-PAGE and stained with Coomassie Blue. The pellet fraction is overloaded 20-fold compared to the total and supernatant fractions. n = 2 biological replicates.

DOI: 10.7554/eLife.19105.015

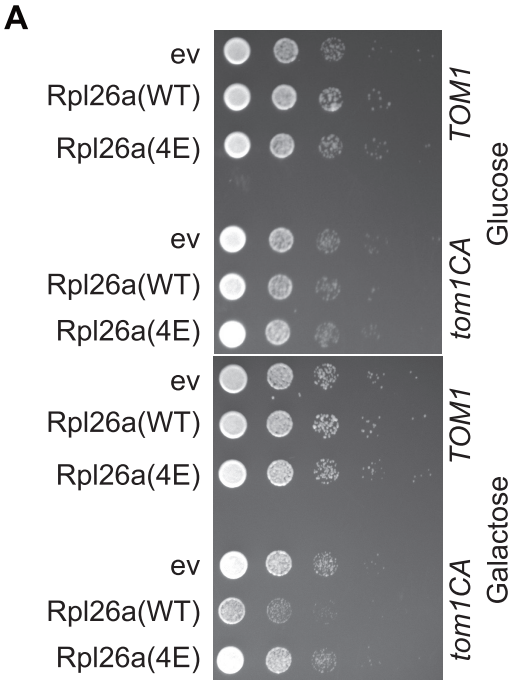

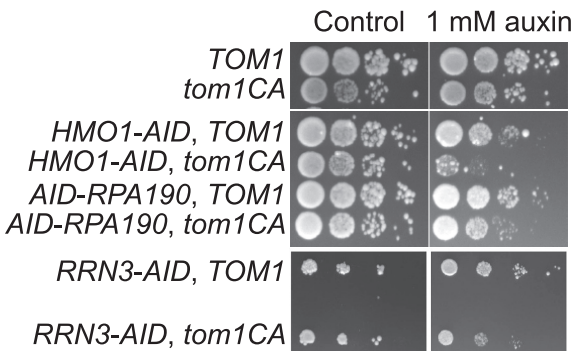

C

Group	Gene	Genetic interaction with *tom1*Δ
Ribosomal Proteins	*RPL2A, RPL6B, RPL8A, RPL9B, RPL11B, RPL13A, RPL16A, RPL17B, RPL23A, RPL24A, RPL31B, RPL35B, RPL36A, RPL37A, RPL40A/B, RPL43B, RPS0A/B, RPS1A, RPS4B, RPS6B, RPS7B, RPS10B, RPS11B, RPS14A, RPS16A/B, RPS21A, RPS22B, RPS23A, RPS24A, RPS27A, RPS29A, RPS30A/B*	Double mutant exhibits reduced growth relative to either single mutant
Stress response	*MSN2, SSB1/2*	Overexpression suppresses *tom1*Δ
PKA	*CYR1, SCH9*	Deletion suppresses *tom1*Δ
	BCY1, PDE2	Overexpression suppresses *tom1*Δ

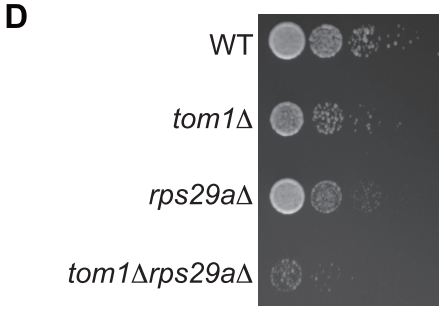

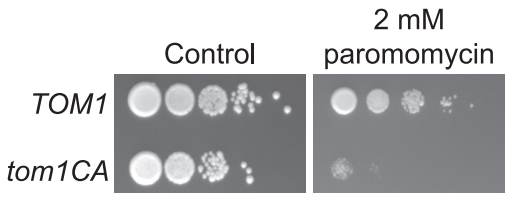

Figure 6—figure supplement 1. Tom1 is required for maintaining proteostasis. (**A**) Cells of the indicated genotypes were spotted in serial 10-fold dilutions on glucose or galactose medium and incubated at 30˚C for 2 days. ev refers to empty vector. n = 2 biological replicates. (**B**) Cells of the

Figure 6—figure supplement 1 continued on next page

Figure 6—figure supplement 1 continued

indicated genotypes were spotted as serial 10-fold dilutions on YPD with or without 1 mM auxin and incubated at 30°C for 2 days. *AID* refers to auxin-inducible degron and *CA* refers to the Cys3235Ala mutation in *TOM1*. n = 2 biological replicates. (**C**) List of genetic interactions with *tom1*Δ as reported in the Saccharomyces Genome Database (www.yeastgenome.org). (**D**) Synthetic growth defects of *rps29a*Δ*tom1*Δ double mutants. Cells of the indicated genotypes were spotted in serial 10-fold dilutions on YPD and incubated at 30°C for 2 days. n = 2 biological replicates. (**E**) same as panel B except medium was supplemented or not with 2 mM paromomycin.

DOI: 10.7554/eLife.19105.016

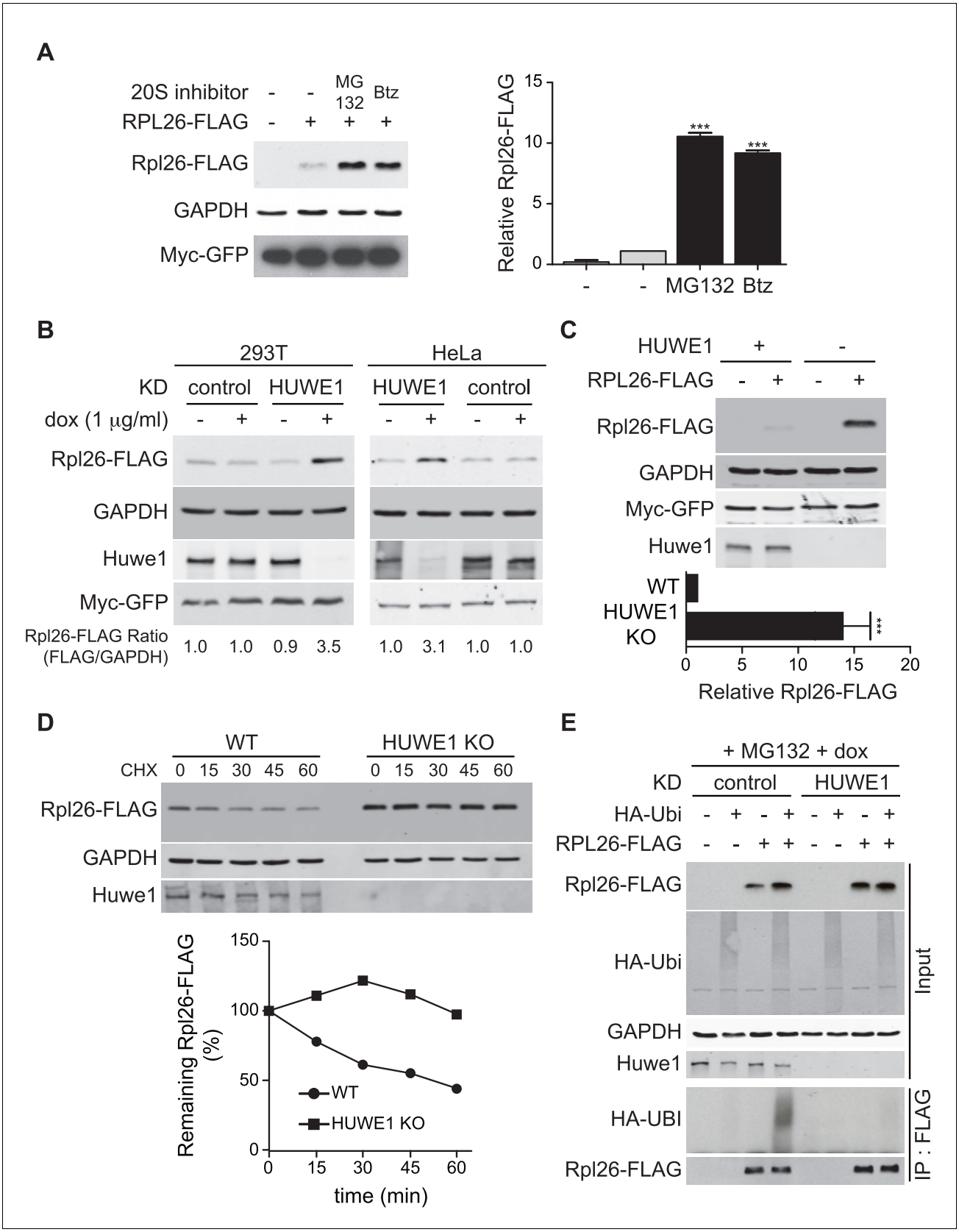

Figure 7. ERISQ is conserved in human cells. (**A**) Proteasome inhibition enables overexpression of human Rpl26. Left: transiently expressed hRpl26^{FLAG} in T-REx-293 cells treated with 10 μM MG132 or 1 μM bortezomib (btz) for 3 hr. Right: quantification of blots. Values are the mean of three independent

Figure 7 continued on next page

Figure 7 continued

experiments and error bars indicate standard deviations. Asterisks indicate significant differences (two-tailed student's t-test, ***p<0.0001, compared with DMSO treatment). n = 3 biological replicates. Source data are available in ***Figure 7—source data 1***. (**B**) Depletion of HUWE1 enables overexpression of human Rpl26. As in (**A**) except that T-REx-293 (left) and HeLa (right) cells were induced with doxycycline for 3 days to express stably integrated shControl or shHUWE1. The relative ratio of $hRpl26^{FLAG}$/GAPDH is shown below each lane. n = 3 biological replicates. Source data are available in ***Figure 7—source data 2***. (**C**) Knockout of *HUWE1* enables overexpression of human Rpl26. Upper: as in (**A**) except that wild type and *HUWE1* knockout HEK293T cells were used. Bottom: quantification of blots. Values are the mean of three independent experiments and error bars indicate standard deviations. Asterisks indicate significant differences (two-tailed student's t-test, ***p<0.0001, compared with WT cells). n = 3 biological replicates. Source data are available in ***Figure 7—source data 3***. (**D**) Overexpressed human Rpl26 is stable in *HUWE1* knockout cells. Upper: wild type and *HUWE1* knockout HEK293T cells transiently expressing $hRpl26^{FLAG}$ were treated with 10 μg/ml cycloheximide (CHX). Bottom: quantification of blot. n = 1 biological replicate. Source data are available in ***Figure 7—source data 4***. (**E**) HUWE1 promotes ubiquitination of overexpressed human Rpl26. As in (**B**) except that ^{HA}ubiquitin was co-expressed with $Rpl26^{FLAG}$ and MG132 was added 3 hr prior to cell lysis. Total cell extract prepared under denaturing condition was adsorbed to FLAG resin and the bound fraction was immunoblotted with antibodies against FLAG and HA. n = 2 biological replicates.

DOI: 10.7554/eLife.19105.017

The following source data is available for figure 7:

Source data 1. Quantification of hRpl26-FLAG and GAPDH levels from three biological replicates.

DOI: 10.7554/eLife.19105.018

Source data 2. Quantification of hRpl26-FLAG and GAPDH levels from one biological replicate.

DOI: 10.7554/eLife.19105.019

Source data 3. Quantification of hRpl26-FLAG and GAPDH levels from three biological replicates.

DOI: 10.7554/eLife.19105.020

Source data 4. Quantification of hRpl26-FLAG and GAPDH levels from one biological replicate.

DOI: 10.7554/eLife.19105.021